BJR https://doi.org/10.1259/bjr.20230704

Received: 31 July 2023 | Accepted: 05 September 2023 | Published online: 24 October 2023

Cite this article as:
Tingen HSA, van Praagh GD, Nienhuis PH, Tubben A, van Rijsewijk ND, ten Hove D, et al. The clinical value of quantitative cardiovascular molecular imaging: a step towards precision medicine. *Br J Radiol* (2023) 10.1259/bjr.20230704.

REVIEW ARTICLE

The clinical value of quantitative cardiovascular molecular imaging: a step towards precision medicine

[1]HENDREA SANNE ALETTA TINGEN, MD, [1]GIJS D. VAN PRAAGH, MSc, [1]PIETER H. NIENHUIS, BSc, [2]ALWIN TUBBEN, MD, [1]NICK D. VAN RIJSEWIJK, MD, [1]DERK TEN HOVE, MD, [3]NOUF A. MUSHARI, MSc, [1]T. SAMARA MARTINEZ-LUCIO, MD, [1]OSCAR I. MENDOZA-IBAÑEZ, MD, [1]JOYCE VAN SLUIS, PhD, [1,4]CHARALAMPOS TSOUMPAS, PhD, [1]ANDOR W.J.M. GLAUDEMANS, MD, PhD and [1,5]RIEMER H.J.A. SLART, MD, PhD

[1]Department of Nuclear Medicine and Molecular Imaging, University Medical Centre Groningen, Groningen, The Netherlands
[2]Department of Cardiology, University Medical Centre Groningen, Groningen, The Netherlands
[3]Leeds Institute of Cardiovascular and Metabolic Medicine, University of Leeds, Leeds, United Kingdom
[4]Faculty of Engineering and Physical Sciences, University of Leeds, Leeds, United Kingdom
[5]Biomedical Photonic Imaging Group, Faculty of Science and Technology, University of Twente, Enschede, The Netherlands

Address correspondence to: Mrs Hendrea Sanne Aletta Tingen
E-mail: *h.s.a.tingen@umcg.nl*

The authors Hendrea Sanne Aletta Tingen and Gijs D. van Praagh contributed equally to the work.

ABSTRACT

Cardiovascular diseases (CVD) are the leading cause of death worldwide and have an increasing impact on society. Precision medicine, in which optimal care is identified for an individual or a group of individuals rather than for the average population, might provide significant health benefits for this patient group and decrease CVD morbidity and mortality. Molecular imaging provides the opportunity to assess biological processes in individuals in addition to anatomical context provided by other imaging modalities and could prove to be essential in the implementation of precision medicine in CVD. New developments in single-photon emission computed tomography (SPECT) and positron emission tomography (PET) systems, combined with rapid innovations in promising and specific radiopharmaceuticals, provide an impressive improvement of diagnostic accuracy and therapy evaluation. This may result in improved health outcomes in CVD patients, thereby reducing societal impact. Furthermore, recent technical advances have led to new possibilities for accurate image quantification, dynamic imaging, and quantification of radiotracer kinetics. This potentially allows for better evaluation of disease activity over time and treatment response monitoring. However, the clinical implementation of these new methods has been slow. This review describes the recent advances in molecular imaging and the clinical value of quantitative PET and SPECT in various fields in cardiovascular molecular imaging, such as atherosclerosis, myocardial perfusion and ischemia, infiltrative cardiomyopathies, systemic vascular diseases, and infectious cardiovascular diseases. Moreover, the challenges that need to be overcome to achieve clinical translation are addressed, and future directions are provided.

INTRODUCTION

Cardiovascular diseases (CVD) are a heterogeneous group of diseases and are the primary cause of death globally with rising incidence and mortality rate.[1] Early diagnosis and improved treatment of CVD may lead to better patient care and reduce costs and societal impact.

Precision medicine is an approach to medicine which aims to identify optimal care for an individual or group of individuals rather than for the average population and to distribute medical tests and treatments accordingly.[2] It has the potential to improve health outcomes and transform prevention and treatment options in all medical fields including CVD.[2] Quantitative tomographic imaging of molecules may serve a critical role in the shift towards this approach. Positron emission tomography (PET) and single-photon emission computed tomography (SPECT) provide molecular information in addition to the anatomical context provided by computed tomography (CT) or magnetic resonance imaging (MRI). However, visual assessment is currently primarily the standard of clinical practice, although in research settings quantitative analysis of PET, or with SPECT, demonstrated to be superior to visual assessment of molecular images for multiple indications.[3–6]

Quantitative PET and SPECT may enhance possibilities for screening, early diagnosis, therapy prediction, guiding treatment and assessing likelihood of disease recurrence.[7,8] Recent technical advances in molecular imaging, such as the long axial field-of-view (LAFOV) PET system, use of artificial intelligence (AI), and development of new radiotracers may have tremendous impact on the field once clinical implementation has been achieved. It is crucial to know the challenges that may cause delay in clinical implementation and standardisation of these new techniques and methods, as well as to improve their precision and accuracy.[8–10]

This review aims to provide an overview of the latest advances in quantitative cardiovascular molecular imaging and to identify which obstacles are to be overcome to allow for reproducible, standardised, and reliable incorporation into clinical practice.

QUANTIFICATION METHODS AND CAMERA TYPES

Quantitative metrics

Current recommendations for clinical use of PET and SPECT images in cardiovascular diseases suggest visual interpretation using intensity grades against another region/organ (*e.g.,* liver or ribs), or description of defect size and depth.[9] Conversely, image parameters such as standardised uptake value (SUV) and target-to-background ratio (TBR) are obtained by placing volumes of interest (VOI) at specific locations in the image (Table 1). The SUV is most used as a surrogate of metabolic activity for uptake quantification.[11] In coronary artery disease (CAD), standardised quantitative parameters, *i.e.,* myocardial blood flow (MBF) and coronary flow reserve (CFR), are clinically routinely used already. Other quantification methods are extensively being studied.[12–14]

The simplicity of static scan metrics explains their widespread application; however, measurements are vulnerable to bias.[15,16] Standardisation and harmonisation methods can mitigate SUV bias to a great extent but are not able to account for changes in plasma kinetics or distinguish between specific and non-specific uptake. Both PET and SPECT can be used not only to measure the concentration of the administered radiotracer *in vivo* but also how fast the radiotracer travels within the various body regions, which is essential in studying pharmacokinetic behaviour *in vivo*. Dynamic imaging can include this information as spatiotemporal

Table 1. Quantification PET and SPECT metrics used in cardiovascular diseases

Quantification method	Description
Visual analysis	Visual scoring system is mainly based on a grading scale (*e.g.,* 0 to 3, ranging from normal to intense uptake or a deep defect) by comparing intensity grades of the organ of interest against a background (liver, ribs)
SUV_{mean}	The average uptake within a VOI
SUV_{max}	The highest uptake of a single voxel within a VOI
SUV_{peak}	The highest average uptake in a 1 ml sphere within a VOI
SUV_{total}	The sum of SUV in (multiple) VOI(s). For cardiac sarcoidosis 13 cardiac segments are used[a]
CAA/TLG	Multiplication of the VOI volume with the SUV_{mean} within that VOI. When calculated in amyloidosis, this metric is called the cardiac amyloid activity (CAA). When calculated in [^{18}F]FDG PET, this metric is referred to as total lesion glycolysis (TLG).
TBR[b]	The SUV_{max} of a VOI in the target region divided by the SUV_{mean} of a VOI in a background region (superior/inferior vena cava (*i.e.,* blood pool) or liver)
Patlak	An image derived input function is extracted from the dynamic images by placing a VOI in the ascending aorta. To obtain parametric images from which the Ki and total blood distribution volume can be derived, voxel-wise Patlak analysis is performed using the IDIF and PET time activity curves as input
MBF	Quantitative, automatic, software-based value that correlates both with the basal (MBF in rest) and hyperaemic (MBF in stress) blood flow supply to the myocardial tissue
CFR	Ratio of MBF in stress to MBF in rest
RI	The percentage of increase or decrease in SUV between two time points in a VOI. Typically calculated by subtracting the early SUV from the delayed SUV, dividing this difference by the early SUV and subsequently multiplying it by 100
ACCS	Mean Na[^{18}F]F SUV in the entire heart (segmentation acquired with an AI segmentation model)
CMA	Automated analysis of the total activity of voxels with a SUV higher than a predetermined threshold to define metabolically active tissue in a VOI
CMV	Automated analysis of the total volume of voxels with a SUV higher than a predetermined threshold to define metabolically active tissue in a VOI
%ID	Measured activity in a VOI expressed as a percentage of the total injected tracer dose

ACCS = Alavi-Carlsen calcification score, CAA = cardiac amyloid activity, CFR = coronary flow reserve, CMA = cardiac metabolic activity, CMV = cardiac metabolic volume; MBF = myocardial blood flow, RI = retention index,SUV = standardised uptake value, TBR = target-to-background ratio, TLG = total lesion glycolysis, VOI = volume of interest.

[a]It is not specified which values are summed, i.e., sum of all voxels or a sum of SUV_{mean} from all segments.

[b]The blood pool is often recommended as background for vascular targets to compensate for radiotracer activity in the lumen.

activity concentration measurement is used providing voxel-wise (metabolic) information, *e.g.,* by applying Patlak analysis to obtain the net influx rate constant (K_i).[15,17,18] Parametric images take into account plasma kinetics as well as additional information by deleting non-specific contributions to the PET signal, enabling for instance easier visual detection of small hotspots, particularly in tissues with high background uptake.[19,20] Therefore, dynamic imaging using PET and SPECT can provide superior knowledge of kinetics and may be even more important in precision medicine than static imaging.

Recent advances in PET technology

The adoption of solid-state technology in PET in the last decades has replaced conventional photomultiplier tube (PMT)-based detectors by silicon photomultiplier (SiPM)-based detectors.[16] Consequently, time-of-flight (ToF) has improved coincidence timing resolution to about 200 ps which is expected to enhance even further (100 ps), resulting in superior image quality and therefore more accurate and potentially earlier detection of CVD.[16]

Regarding PET system design, the latest development has been the introduction of LAFOV PET systems (Figure 1).[21] These systems surround the patient with a substantially increased number of detectors axially, resulting in significantly improved sensitivity and larger anatomical and multi-organ coverage.[22–24] LAFOV PET comes with numerous unexplored opportunities for research and clinical applications, such as the evaluation of organ crosstalk including the cardiovascular system.[21,25,26]

Besides acquisition technology, several other factors influence quantification of CVD including reconstruction algorithms and settings.[27] Iterative reconstruction algorithms have replaced filtered back projection for clinical routine. Herein, application of resolution modelling improves signal-to-noise ratio and contrast. A large number of iterations improves quantitative accuracy but also increases noise which influences precision.[28] To decrease noise, post-reconstruction (Gaussian) smoothing is usually applied, which may improve signal-to-noise, but decreases contrast.[29] New iterative reconstruction methods that use prior information from CT[30] or MRI[31] images could be utilised to reduce noise and harmonise and standardise the images to eliminate overiteration.

Another technological achievement of the past decade was the development of PET/MRI which has the advantage of imaging the cardiovascular system with more detail and scrimps on radiation exposure. This gives the opportunity to combine PET quantification with more detailed heart or vessel measurements on MRI.[32] Newest generation PET/MRI systems use SiPM detectors that pave the way for ToF-based imaging.[32]

PET/MRI systems can be also powerful in detecting motion using MRI and correcting for it in PET, enabling even higher resolution in the cardiac region. Cardiac motion correction for PET/CT is not routinely performed, but is available in digital systems using electrocardiogram gating, optionally combined with respiratory gating. Cardio(respiratory) motion correction may result in increased signal efficacy and more accurate image reconstruction, but large prospective studies are still needed.

Recent advances in SPECT technology

A growing number of nuclear medicine sites is using a new generation of cardiac-centred SPECT for myocardial imaging. The conventional sodium iodine (NaI) crystals used for the detection of γ rays have been replaced by cadmium-zinc-telluride (CZT). This crystal transforms the signal induced by γ rays directly into electric impulses without the need of photodetectors. CZT provides a four to sevenfold higher system sensitivity compared to NaI-based cameras,[33] which allows for a substantial decrease in radiopharmaceutical injection activity in combination with faster acquisition time. However, its clinical added value still needs confirmation.[14,34] Additionally, dedicated cardiac SPECT offers the opportunity for dynamic scanning of the heart.

Artificial intelligence

AI may help improve quantification of CVD in various methods: *e.g.,* reconstruction, denoising, partial volume correction, motion compensation, image registration, image segmentation, and automated quantification.[10] All of them are intertwined and play their own role in quantification.

The bottleneck of laborious, time-consuming, and prone-to-variability manual segmentation can be alleviated by AI.[35] Multiple AI models have recently been published to segment the heart and some large vessels in PET and/or CT (Figure 2).[36,37] This could speed up quantitative research in cardiovascular diseases tremendously and potentially provide accurate and standardised quantitative analyses of these diseases for primary diagnosis and disease monitoring. Deep learning or radiomics in combination with machine learning can be used in decision-making and disease monitoring of CVD. It can use both image data as well as clinical biomarkers. This would enhance precision phenotyping and more accurate classification of diseases and thus potentially a better understanding of diseases.[38]

CARDIOVASCULAR DISEASES

Implementation of all of the above in daily clinical practice is largely still lacking. We will now provide an overview of the possibilities where quantification offers in specific cardiovascular diseases (atherosclerosis, coronary artery disease, cardiac amyloidosis and sarcoidosis, and in cardiovascular inflammation and infection), and we will describe the current use of quantification in daily practice. This review will not focus on the various radiotracers used in the different disease; however, an overview of studied and clinically used radiotracers is provided in Table 2.

Atherosclerosis

Atherosclerosis is a chronic inflammatory condition marked by formation of fibrofatty lesions in arterial walls. Calcium mineralization in the atherosclerotic artery further solidifies plaque formation causing narrowing of the vessel.[39] Several studies have shown the potential of PET technology using [^{18}F]FDG or particularly Na[^{18}F]F as early markers for cardiovascular disease or adverse events.[40–43] The combination of metabolic imaging through PET in anatomical context enables earlier risk

Figure 1. Illustrative image regarding dynamic PET acquisition and parametric image analysis using an LAFOV PET/CT system in cardiovascular disease. Dynamic imaging was performed using an LAFOV PET/CT scanner with a 106 cm field-of-view in this patient with suspected vasculitis. A 65 min dynamic acquisition was started simultaneously with the intravenous injection of [^{18}F]FDG. PET data were reconstructed using 31 frames as follows: 6 × 10 sec, 3 × 20 sec, 6 × 30 sec, 5 × 1 min and 11 × 5 min. Series A through D shows different frames: frame 4, 30–40 sec (a), frame 15, 270–300 sec (b), frame 23, 20–25 min (c) and frame 31, 60–65 min (d). In D, arrows indicate three regions suspicious for vasculitis: red for the ascending aorta, green for the aortic arc and blue for the carotid artery. E shows the time activity curve for the different volumes of interest: the three vasculitis regions, the liver reference region and the descending aorta (which is also the image derived arterial input curve). F shows a schematic of Patlak linearisation using the image derived input curve from the descending aorta and the different tissue time activity curves from E to obtain the net influx rate (Ki). G shows the parametric Ki image, in H you can see the segmented VOIs. LAFOV = long axial field of view, [^{18}F]FDG = 2-deoxy-2-[^{18}F]fluoro-D-glucose, PET = positron emission tomography, Ki = tracer net influx constant, VOI = volume of interest.

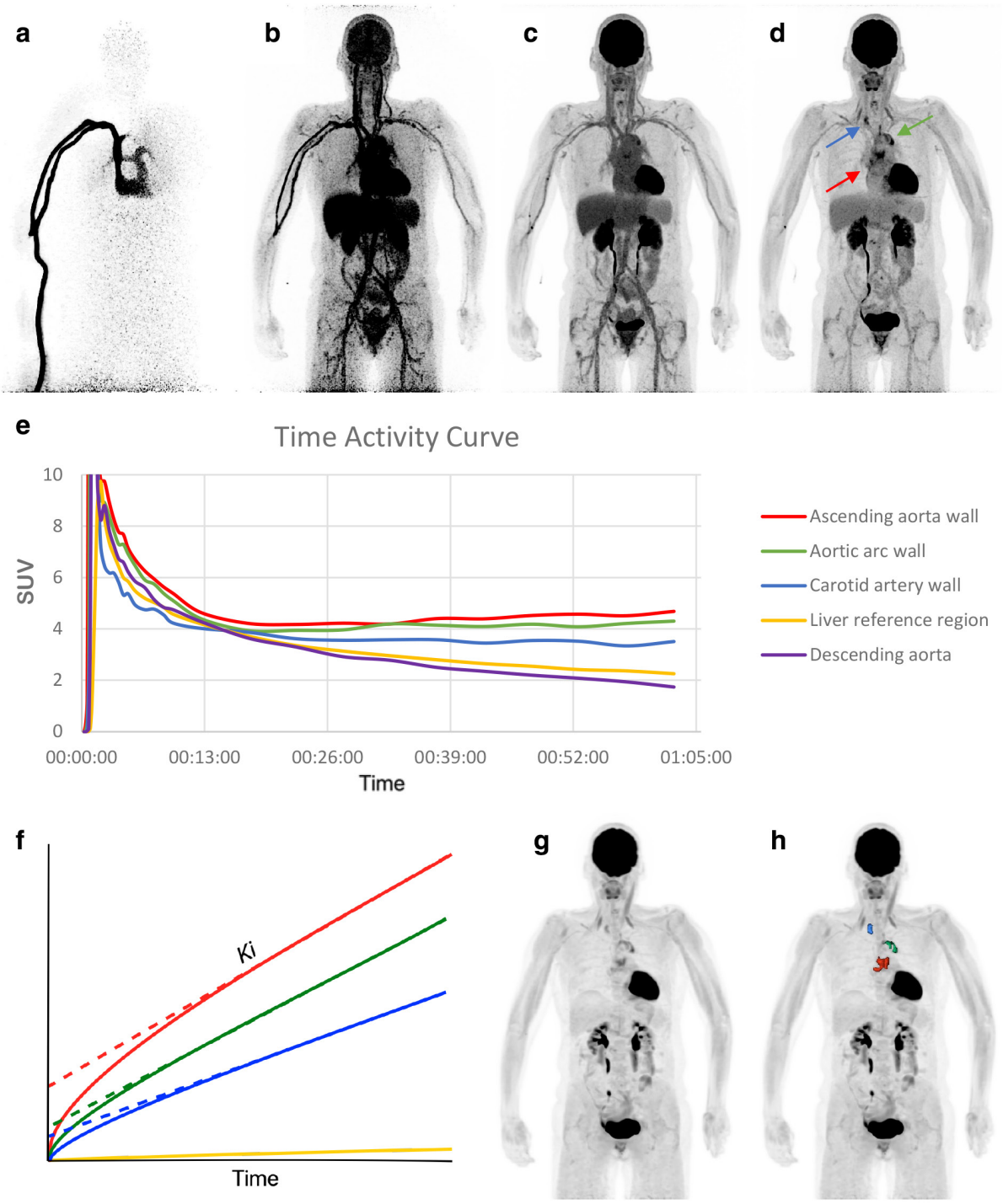

Figure 2. Example output of the cardiovascular system from an artificial intelligence segmentation model. Different sections of the cardiovascular system can be segmented from CT scans. These segmentations can be used to quantify radiotracer uptake in the specific regions. This may possibly speed up quantitative research in cardiovascular diseases tremendously and potentially provide accurate and standardised quantitative analyses of these diseases for primary diagnosis and disease monitoring. Output results should be properly checked and adjusted if needed (see iliac artery). Segmentations are acquired with a previously published, open-source AI model from Wasserthal et al.[36] AI = artificial intelligence.

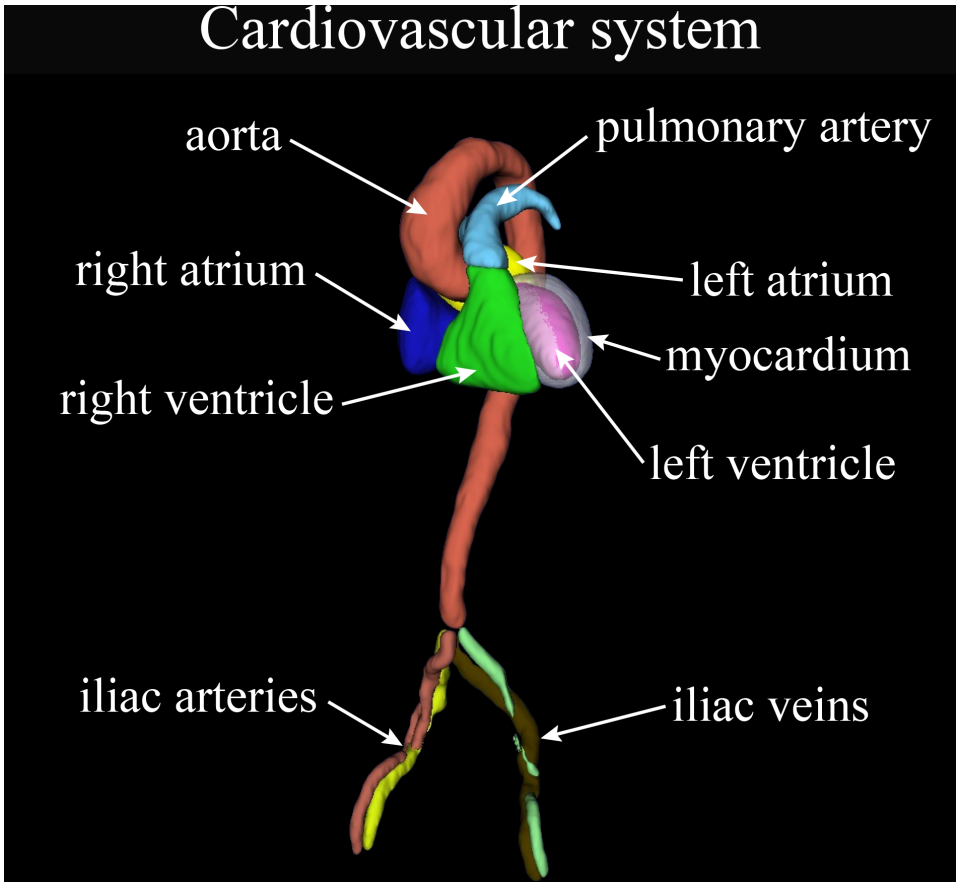

assessment than current late-stage atherosclerotic imaging used for risk profiling.[44]

Multiple quantitative metrics have been used, such as SUV_{max}, SUV_{mean}, TBR_{max}, the Alavi-Carlsen calcification score (ACCS), and the coronary microcalcification activity (CMA).[44–47] The common metrics (SUV_{max} and TBR) are prone to image noise and manual error. The ACCS uses AI segmentation of the entire heart to calculate the mean SUV of Na[^{18}F]F uptake.[46] The CMA is a similar score using Na[^{18}F]F to measure both the per vessel and per patient plaque burden.[47] In a retrospective cohort, patients with a CMA of 0 had 0% incidence of fatal or non-fatal myocardial infarction. A CMA threshold of 1.56 may identify high-risk patients as higher values were associated with an over sevenfold increase in the incidence of myocardial infarction.[48] When interpreting above scores, it should be considered that uptake of [^{18}F]FDG and Na[^{18}F]F could also be caused by other diseases, like vasculitis or cardiac amyloidosis, as described later in this review.

CT is still acknowledged as the most accurate and reliable modality for quantification of stenosis and coronary plaque burden.[49] PET could prove useful in clinical practice for imaging of vulnerable plaques with improved spatial resolution and reduced motion artefacts, but more clinical trials are needed. In combination with MRI, content of plaques could potentially be evaluated while PET tracers could assess the degree of plaque activity.[50] Furthermore, LAFOV PET provides the opportunity of dynamic imaging and kinetic modelling not only in the coronary arteries but also in larger vessels. This gives the potential to quantify total body microcalcification activity burden.[42,44] Besides, a direct comparison between vessels can be made, which would be of great interest as the morphological characteristics of atherosclerotic plaques and their stability vary across the vascular tree.[51] However, robust, automated segmentation models of the vascular tree are pivotal for this application as manual segmentation would be too labour intensive. Total body microcalcification activity scores could improve personalised risk assessment and monitoring.[41] Furthermore, since the 2016 European Association of Nuclear Medicine (EANM) position paper, no major changes in standardisation or recommendations have been done for molecular atherosclerotic imaging and an update of is needed.[45]

Table 2. Radiopharmaceuticals used in specific diseases

Radiopharmaceuticals	Abbreviation
Atherosclerosis	
PET	
2-deoxy-2-[^{18}F]fluoro-D-glucose	[^{18}F]FDG
Sodium [^{18}F]fluoride	Na[^{18}F]F
Coronary artery disease	
SPECT	
[^{99m}Tc]−2-methoxyisobutylisonitrile	[^{99m}Tc]-sestamibi
[^{99m}Tc]−1,2-bis[bis(2-ethoxyethyl) phosphino] ethane	[^{99m}Tc]-tetrofosmin
(^{201}Tl)thallium monochloride	[^{201}Tl]Cl
PET	
Rubidium-82	^{82}Rb
[^{13}N]ammonia	[^{13}N]NH_3
[^{15}O]water	[^{15}O]H_2O
[^{18}F]flurpiridaz	[^{18}F]flurpiridaz
Sodium [^{18}F]fluoride	Na[^{18}F]F
^{68}Ga]-fibroblast activation protein inhibitor 04	[^{68}Ga]FAPI-04
[^{124}I]-amyloid-reactive peptide	[^{124}I]AT-01
Cardiac amyloidosis	
SPECT	
[^{99m}Tc]-pyrophosphate	[^{99m}Tc]Tc-PYP
[^{99m}Tc]−3,3-diphosphono-1,2–2-propanodicarboxylic acid	[^{99m}Tc]Tc-DPD
[^{99m}Tc]-hydroxy-methylene-diphosphonate	[^{99m}Tc]Tc-HDP
[^{123}I]-meta-iodobenzylguanidine	[^{123}I]mIBG
PET	
[^{11}C]-Pittsburgh compound B	[^{11}C]PIB
[^{18}F]-Florbetaben	[^{18}F]FBB
[^{18}F]-Florbetapir	[^{18}F]FBP
[^{18}F]-Flutemetamol	[^{18}F]FMM
Sodium [^{18}F]fluoride	Na[^{18}F]F
[^{68}Ga]-fibroblast activation protein inhibitor 04	[^{68}Ga]FAPI-04
[^{124}I]-amyloid-reactive peptide	[^{124}I]AT-01
Cardiac sarcoidosis	
SPECT	
[^{67}Ga]-citrate	[^{67}Ga]-citrate
[^{99m}Tc]−2-methoxyisobutylisonitrile	[^{99m}Tc]-sestamibi
[^{99m}Tc]−1,2-bis[bis(2-ethoxyethyl) phosphino] ethane	[^{99m}Tc]-tetrofosmin
PET	
2-deoxy-2-[^{18}F]fluoro-D-glucose	[^{18}F]FDG
[^{13}N]ammonia	[^{13}N]NH_3
[^{68}Ga]-DOTA-Tyr(3)-Thr(8)-octreotate	[^{68}Ga]-DOTATATE
[^{68}Ga]-DOTA-NaI-octreotide	[^{68}Ga]-DOTANOC

(Continued)

Table 2. (Continued)

Radiopharmaceuticals	Abbreviation
[^{68}Ga]-DOTA-Tyr-octreotide	[^{68}Ga]-DOTATOC
[^{11}C]palmitate	[^{11}C]palmitate
[^{18}F]-fluoromisonidazole	[^{18}F]-FMISO
[^{68}Ga]- / [18F]-fibroblast activation protein inhibitor 04	[^{68}Ga]FAPI-04 / [18F]FAPI-04
3′-deoxy-3′-[^{18}F]fluorothymidine	[^{18}F]FLT
Large vessel vasculitis	
2-deoxy-2-[^{18}F]fluoro-D-glucose	[^{18}F]FDG
Cardiovascular infection	
2-deoxy-2-[^{18}F]fluoro-D-glucose	[^{18}F]FDG
[^{99}mTc]-leucocytes / [^{111}In]-leucocytes	WBC

PET, positron emission tomography; SPECT, single-photon emission computed tomography.

Coronary artery disease

In CAD, atherosclerotic plaques narrow or obstruct coronary arteries, impairing heart oxygenation, and causing diverse clinical syndromes (*i.e.,* (un)stable angina and myocardial infarction).[52] Invasive coronary angiography was commonly used for CAD evaluation in the past, but recent trials have shown that not all patients benefit from this approach.[53,54] Molecular imaging modalities offer a non-invasive way to assess heart perfusion, improving evaluation, stratification, and prognosis.

Currently, the non-invasive gold-standard metrics for myocardial perfusion are the myocardial blood flow (MBF) at rest and stress, and coronary flow reserve (CFR). These metrics are proven to correlate with the basal and hyperaemic blood flow supply, and blood flow augmentation in response to increased contractility requirements, respectively.[55] However, conventional SPECT systems do not provide accurate tracking of tracer concentration over time.[56] This limits clinical evaluation to visual assessment and suboptimal quantitative metrics (*e.g.,* summed rest score) that estimate the presence and burden of ischemic and infarcted tissue.[7] New generation devices with solid-state detectors (CZT SPECT) offer improved sensitivity and spatial resolution, enabling more accurate estimation of MBF and CFR with preliminary results comparable to the current gold standard.[57,58]

MBF and CFR values are already routinely estimated on PET.[59] However, the precision and reproducibility vary depending on the radiotracer used. Although[60] Rb is the most common tracer, it has a suboptimal non-linear relationship with MBF.[61] On-site ("mini") cyclotrons and dedicated PET systems could facilitate the use of tracers with better kinetics such as [^{15}O]H_2O and [^{13}N]NH_3.[13,62]

Another critical challenge for quantification of CAD is cardiac and respiratory motion artefacts, in addition to whole body motion. These factors cause misalignment between cardiac CT/MRI and cardiac PET images, leading to inaccurate estimation of time activity curves and image-based arterial input function. At the moment, no validated generic methodology exists to overcome motion in dynamic imaging, necessitating further research in this area.[63]

Cardiac amyloidosis

In cardiac amyloidosis (CA), misfolded proteins progressively deposit in the extracellular matrix. The most common types are light chain (AL) and transthyretin (ATTR) amyloidosis.[64] Recently, treatment options for ATTR amyloidosis patients with cardiomyopathy (ATTR-CA) have expanded,[65] necessitating accurate assessment methods for disease progression and treatment response, like quantitative molecular imaging, to guide therapy.

Bone scintigraphy is currently the only molecular imaging modality clinically used in CA and is considered the cornerstone of non-invasive diagnosis of ATTR-CA.[64] Although several cardiac TBRs on planar images have been studied, only visual scoring is used in clinical practice.[64,66] To overcome the influence of extracardiac radiotracer uptake on TBRs on planar images, efforts have been made to perform quantified SPECT.[4,12] Recent studies suggest quantified SPECT provides clinically relevant results and might outperform planar quantification techniques.[3,4] Additionally, therapy-related changes in cardiac radiotracer uptake have been detected using SPECT quantification,[67–69] while visual scoring was deemed unsuitable for this purpose[70] (Figure 3).

Quantitative bone scintigraphy may pave the way for quantitative [^{123}I]mIBG scintigraphy. [^{123}I]mIBG is used to assess cardiac denervation in a research setting[72] but is currently only quantified by calculating TBRs on planar images,[72] similar to bone scintigraphy.

For clinical implementation of quantified SPECT in CA, regular quality controls incorporating a national institute of standards and technology (NIST) traceable calibration source should be performed in all centres to ensure interinstitutional reproducibility in measurements.[73] Next, reproducibility and implications

Figure 3. Example case of a serial [^{99m}Tc]-DPD bone scintigraphy in a wild type ATTR amyloidosis patient. Whole body anterior planar images before (a) and after (d) 6 months treatment with 61 mg tafamidis and quantitative SPECT/CT scans before (b) and after (c) treatment. Visual assessment of planar images suggests a decrease in cardiac tracer uptake despite unchanged Perugini score, this decrease is reflected by a decrease in myocardial SUV_{max} and myocardial TBR on quantified SPECT scans indicating the potential of quantified SPECT in the follow-up of patients compared to visual assessment of planar images. This image was adapted from Zhao, et al[71] and reprinted under the terms of the Creative Commons CC BY license. DPD = 3,3-diphosphono-1,2-py rophosphate, ATTR = transthyretin amyloid, SPECT = single-photon emission tomography, SUV = standardised uptake value, TBR = target-to-background ratio.

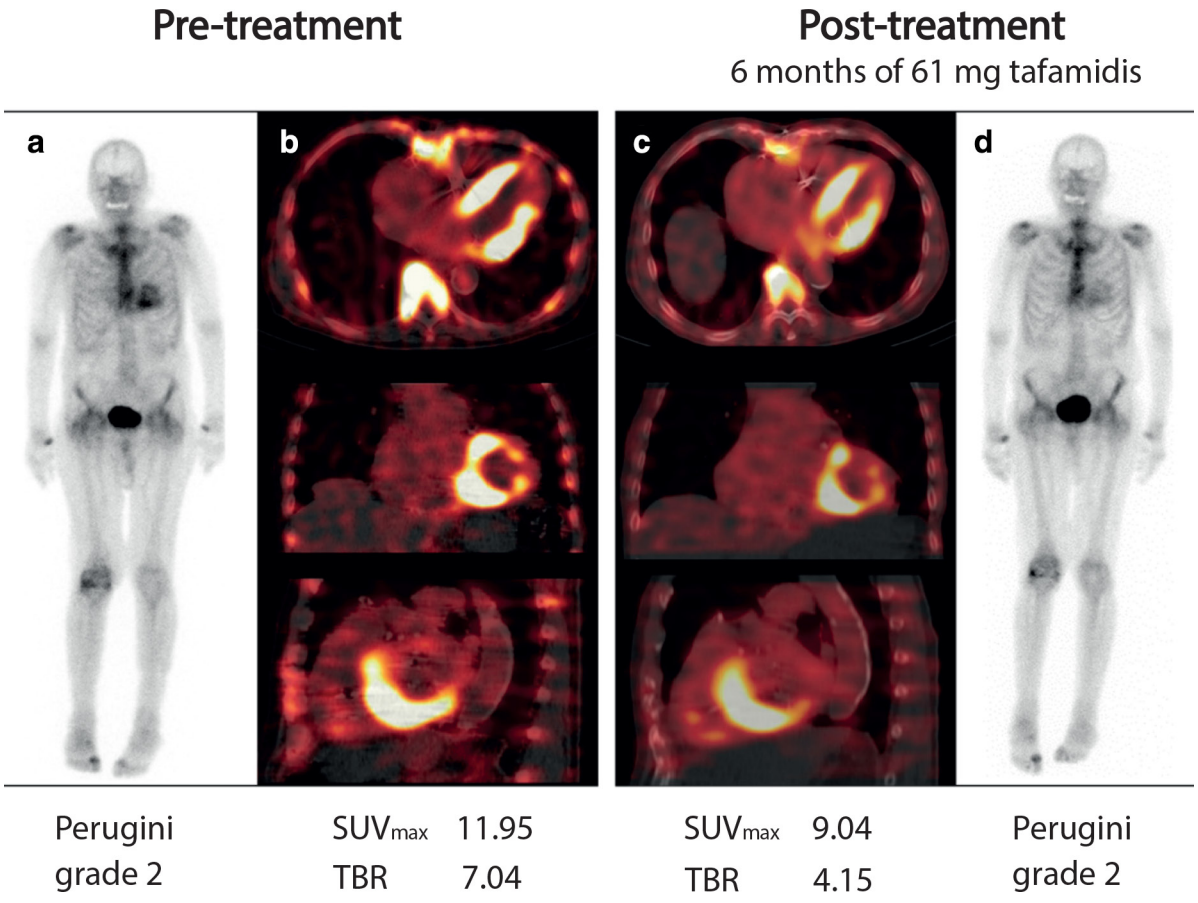

of quantified bone scintigraphy and [^{123}I]mIBG should be evaluated in large multicentre studies.

PET quantification in CA is limited to research settings. Six PET-tracers have been investigated.[74] Retention index (RI), TBR, and SUV_{max} are frequently used measurements to assess amyloid load on static and dynamic PET and can be used to distinguish the subtypes of CA and healthy controls in [^{11}C]PIB[75–79] and Na[^{18}F]F PET.[80–83] Kinetic modelling improved diagnostic accuracy of [^{18}F]FBB-PET for CA in one study using a two-tissue irreversible kinetic model,[60] exceeding results of previous studies.[84,85] Although quantitative PET shows promise for monitoring CA, only two case series with conflicting results have been described.[84,86]

Large multicenter studies are necessary to validate PET in clinical care. Additionally, the effect of kinetic modelling on diagnostic accuracy should be assessed for all studied radiotracers. The effects of cardiac and respiratory motion correction on outcomes should be assessed for quantitative SPECT and PET, as movement artefacts are to be expected in the cardiac region of interest.

Cardiac sarcoidosis

Sarcoidosis is an inflammatory disease that affects multiple organ systems and is characterised by noncaseating granulomas in the affected organs.[5] Clinical diagnosis of cardiac sarcoidosis (CS) is made in approximately 5% of sarcoidosis patients; however, autopsy studies show a much higher prevalence.[87–89] As CS accounts for 13–85% of deaths in sarcoidosis patients, reducing underdiagnosis is crucial to improve outcomes in this group.

Multiple diagnostic criteria and consensus papers are used to diagnose CS, with differing roles for radionuclide imaging.[8,90,91] While visual inspection of [^{67}Ga]-citrate scintigraphy and SPECT was previously used, [^{18}F]FDG PET is now preferred for its higher sensitivity and better spatial resolution.[8] Although it is not recommended as the first-line diagnostic technique, [^{18}F]FDG PET can aid in the staging process by differentiating active

(reversible) lesions from fibrotic (irreversible) lesions and is the first-line imaging modality to assess treatment response.[92]

Apart from visual scoring, various quantitative metrics for [^{18}F]FDG have been studied in CS, such as SUV_{max}, SUV_{mean}, SUV_{total}, Patlak slope *Ki* parameters, TBRs, cardiac metabolic volume (CMV), and cardiac metabolic activity (CMA). While elaborate head-to-head comparisons of these metrics are lacking, data suggest superior performance to visual assessment.[6,91] Combining quantitative metrics with visual assessment is recommended for clinical practice, and SUV_{max} and CMA have been proposed.[8,90]

Combined assessment of [^{18}F]FDG PET and myocardial perfusion imaging (MPI) is currently recommended for disease staging, but may also have a crucial role in the assessment of therapy response in the future. MPI PET is preferred over MPI SPECT for detecting the small perfusion defects present in CS patients.[8] Reduction of SUV_{max} and volume of inflammation (volume of voxels with a SUV_{max} above a predetermined threshold) have been associated with improvement in outcomes[93,94] and a change of ≥20% in both parameters is suggested to be clinically significant.[95] However, further research is required on this topic.[96]

Furthermore, recent [^{18}F]FDG studies indicate improved accuracy for hybrid PET/MRI systems in diagnosing and staging CS patients.[97–99] PET/MRI can be particularly useful for cases where myocardial [^{18}F]FDG uptake suppression fails, as the MRI signal can serve as an alternative evaluation tool. Additionally, multiple radiotracers with no physiological cardiac uptake, such as [^{68}Ga]DOTATOC,[100] are being studied to address the issue of failed myocardial [^{18}F]FDG uptake suppression. Furthermore, the use of radiomics in PET[101] and/or MRI[102] could further enhance automation of analysis, AUC and accuracy. Further studies are needed to explore the role of PET/MRI in CS diagnosis, prognostic staging, and monitoring of therapy response.[8,90,92,103] Additionally, the value of motion correction should be investigated.

Large vessel vasculitis

Large vessel vasculitis (LVV) is a group of diseases that are characterised by inflammation of the large and medium-sized arteries. The main types are giant cell arteritis (GCA) and Takayasu Arteritis (TAK), which typically differ in its localisation and age of onset. Accurate and timely diagnosis are vital in LVV to prevent permanent vascular and end-organ damage. Diagnosis is challenging because there are no disease-specific signs, symptoms, or diagnostic tests. In addition, it is difficult to predict response to therapy and potential adverse effects.

[^{18}F]FDG PET/CT is an established diagnostic tool for LVV, showing increased uptake in the inflamed arterial wall.[104] Typical high-intensity uptake in a circumferential pattern is highly characteristic of LVV. The current recommended method for [^{18}F]FDG uptake intensity is a visual comparison with liver uptake on a 0 to 3 scale.[105] This is the most established method due to its simplicity. However, many other methods, *e.g.,* SUV and TBR measurements, have been described in literature and occasionally show better diagnostic performance.[106] Various background tissues have been evaluated, including the liver, inferior caval vein, superior caval vein, and internal jugular vein. A TBR using the liver SUV_{max} as background may have the highest diagnostic accuracy for LVV, but nonetheless remains inferior to visual assessment.[107] The use of radiomic features and AI may provide a more consistent quantitative assessment approach.[108,109]

Increased uptake on [^{18}F]FDG PET/CT has also been shown to be associated with increased aortic dimensions and a higher risk of aortic complications.[110,111] Additionally, GCA patients may have persistent vascular [^{18}F]FDG uptake during follow-up.[112] Both prognostic imaging and monitoring scans may benefit from quantification as this may allow for more accurate comparison between patients and subsequent scans.

Standardisation of quantitative parameters is vital for the implementation of these parameters into clinical practice. Additionally, manual segmentation of the arterial tree and calculating uptake values is significantly more time-consuming than visual assessment. This could be resolved using future implementation of AI models.

It should be noted that factors such as serum glucose levels, renal clearance, fat mass, and the use of glucocorticoids also influence the outcome in quantitative parameters.[107,113] Besides, atherosclerosis causes increased uptake in the arterial wall as well, making differentiation with LVV challenging.[114] Especially in patient monitoring, these factors influence the diagnostic accuracy of [^{18}F]FDG PET.[115] Future standardised quantitative methods for LVV should account for these factors affecting tracer kinetics.

Cardiovascular infections

Cardiovascular infections encompass a wide range of diseases affecting different parts of blood vessels and the heart, including the endocardium, myocardium, and pericardium,[116] resulting in diverse and potentially nonspecific symptoms.[116,117] Despite therapeutic advancements, cardiovascular infections continue to have a high mortality rate.[117,118] Therefore, prompt and accurate diagnosis is crucial.

Nuclear medicine has an established role in the diagnostic workup and imaging of cardiac infections, such as endocarditis, cardiac device related infections,[118] and vascular graft infections.[117] Frequently used are [^{18}F]FDG PET/CT and white blood cell (WBC) scintigraphy.

In general, interpretation of [^{18}F]FDG PET/CT in cardiovascular infections is based on visual analysis. Focal, heterogeneous uptake, persisting also on the non-attenuation-corrected images, suggests infection. Various quantitative metrics have been studied in diagnosing cardiovascular infections with [^{18}F]FDG PET/CT, including TBR, SUV_{peak}, SUV_{max}, and visual grading scales.[119,120] A meta-analysis found focal uptake and SUV_{max} to be the most accurate indicators of vascular graft infections.[121]

For prosthetic valve endocarditis, results on the use of quantitative metrics are mixed. While some studies have shown high diagnostic accuracy for quantitative metrics,[122,123] visual analysis remains the preferred method of PET/CT analysis for suspected endocarditis. Quantitative metrics may serve as an adjunct in cases of inconclusive visual analysis.

In a recent study for suspected infection of a left ventricular assist device (LVAD), SUV_{max} reliably predicted driveline infections with improved diagnostic accuracy compared with visual analysis. For the central device components, TBR with liver as background showed significantly higher diagnostic accuracy than visual analysis (sensitivity 1.00 *vs* 0.75, specificity 0.80 *vs* 0.60).[124] However, future confirmation is required for standardised use of these metrics in clinical practice.

[^{18}F]FDG is a nonspecific radiotracer unable to differentiate between infection and inflammation on single static images. One small study with dual time point imaging has been performed, suggesting a RI cut-off of >20% to distinguish infection form inflammation in suspected aortic graft infections.[125] Further studies are needed to determine if dynamic imaging or bacteria-specific radiotracers offer added value.

Scintigraphy with radiolabelled WBCs could serve as an alternative to [^{18}F]FDG PET as infection can be distinguished from inflammation by tracking radiotracer uptake over time.[126] When uncertainty persists after visual assessment, quantitative measurements can be performed. An increase in TBR_{mean} by at least 10% over time suggests the presence of an infection.[126]

Large clinical studies are required to validate the utility of quantitative measures in improving the accuracy and efficiency of diagnosis and treatment monitoring for cardiovascular infections. Furthermore, the effect of motion correction should be evaluated.

DISCUSSION & FUTURE PERSPECTIVES

This review aimed to give an overview of the latest advances in quantitative molecular cardiovascular imaging and to identify the challenges to overcome before full clinical implementation is possible. An overview was given of the currently used quantification methods in clinical and research settings and the recent technical advances in acquisition and reconstruction of camera systems. Besides, for each cardiovascular disease the latest developments in terms of quantification and challenges to overcome to implement into clinic were presented.

Radionuclide imaging could be a revolutionary step towards precision medicine. Its ability to look into physiological processes within the body led to new opportunities and continues to have tremendous undiscovered potential. A large challenge in radionuclide imaging is accurate and precise quantification.[7,127] Current clinical recommendations are primarily visual analysis of the images.[9] As shown in this review, for all cardiovascular diseases a tremendous work of research has been done to find the most optimal quantitative parameter for diagnosis, treatment response prediction, and patient monitoring. However, study design and results may greatly vary among studies. Also, the fast-developing technical advances make it even more challenging to properly standardise quantification. Nonetheless, it is essential to standardise quantification methods in cardiovascular molecular imaging for full empowerment of precision medicine.

First of all, to get interscanner and interinstitutional comparable results, it is advised to regularly follow existing procedure guidelines for cardiovascular imaging, including standardised protocols for patient preparation, image acquisition, and reconstruction settings.[9,14,32,59,105,126] Second, we recommend guidelines per cardiovascular disease for standardised quantification in currently used clinical images to increase homogeneity in research and to get strong evidence for precision medicine. Third, possibilities of technical advances should be extensively explored. For example, organ crosstalk with the recently developed LAFOV PET system[21,26]; use of motion correction and ECG-gated reconstruction methods; state-of-the-art PET/MRI systems for quantification of metabolic changes compared to systemic changes in the heart and blood vessels and the use of MR images to compensate for cardiac and respiratory motion[63]; calibration of SPECT systems for quantitative uptake values[13]; and AI to increase the speed of labour-intensive quantification tasks, improve image quality, or reduce the amount of administered radiotracer activity. The EANM, Society of Nuclear Medicine and Molecular Imaging (SNMMI), and European Association of Cardiovascular Imaging (EACVI) also recommend the use of AI and radiomics in studies.[10,128] Automation of time-consuming and prone-to-human-variability steps can lead to more objectively determined parameters. See Table 3 for more items to be addressed for improvement of quantification and implementation into clinical practice. This can be translated in a better understanding of the physiology behind cardiovascular diseases. Clinically, it may give the opportunity to

Table 3. Items to be addressed for improvement of cardiovascular molecular imaging quantification and implementation into clinical practice

1.	Standardisation of quantification methods and parameters per cardiovascular disease in static and dynamic PET and SPECT
2.	Standardisation of calibration methods for quantitative SUV SPECT
3.	Solutions for cardiac and respiratory motion
4.	Exploration of the added value of dynamic imaging in cardiovascular imaging
5.	Use of AI segmentation models in research studies for more robust delineation of the target of interest, including smaller vessel diameters
6.	Evaluation of the added value of (quantitative) hybrid PET/MRI for cardiovascular diseases
7.	Development of cardiovascular disease specific radiotracers

AI = artificial intelligence, MRI = magnetic resonance imaging;PET = positron emission tomography, SPECT = single-photon emission computed tomography, SUV = standardised uptake value.

assess the type and dose of treatment per patient; to predict treatment response of the patient; to evaluate the progression of the patient; and to improve interinstitutional and intermanufacturer quantification.

To conclude, many studies have been done recently to improve quantitative molecular cardiovascular imaging. Besides, technical advances pave the way for more objective, more accurate, and more robust measurements. However, for all cardiovascular diseases it is of utmost importance to get standardised quantitative metrics to achieve more evidence by larger and more homogeneous (prospective) studies and definition of normal and abnormal cut-off values. This will lead to improved stratified precision medicine in terms of improved diagnosis, prediction of treatment response, and patient monitoring.

REFERENCES

1. Tsao CW, Aday AW, Almarzooq ZI, Alonso A, Beaton AZ, Bittencourt MS, et al. Heart disease and stroke Statistics—2022 update: A report from the American heart Association. *Circulation* 2022; **145**: e153–639. https://doi.org/10.1161/CIR.0000000000001052
2. Leopold JA, Loscalzo J. Emerging role of precision medicine in cardiovascular disease. *Circ Res* 2018; **122**: 1302–15. https://doi.org/10.1161/CIRCRESAHA.117.310782
3. Bellevre D, Bailliez A, Delelis F, Blaire T, Agostini D, Mouquet F, et al. Quantitation of myocardial 99Mtc-HMDP uptake with new SPECT/CT cadmium zinc Telluride (CZT) camera in patients with Transthyretin-related cardiac Amyloidosis: ready for clinical use *J Nucl Cardiol* 2022; **29**: 506–14. https://doi.org/10.1007/s12350-020-02274-2
4. Scully PR, Morris E, Patel KP, Treibel TA, Burniston M, Klotz E, et al. DPD Quantification in cardiac Amyloidosis. *JACC: Cardiovascular Imaging* 2020; **13**: 1353–63. https://doi.org/10.1016/j.jcmg.2020.03.020
5. Birnie DH, Nery PB, Ha AC, Beanlands RSB. Cardiac Sarcoidosis. *Journal of the American College of Cardiology* 2016; **68**: 411–21. https://doi.org/10.1016/j.jacc.2016.03.605
6. Ahmadian A, Brogan A, Berman J, Sverdlov AL, Mercier G, Mazzini M, et al. Quantitative interpretation of FDG PET/CT with myocardial perfusion imaging increases diagnostic information in the evaluation of cardiac Sarcoidosis. *J Nucl Cardiol* 2014; **21**: 925–39. https://doi.org/10.1007/s12350-014-9901-9
7. Giardino A, Gupta S, Olson E, Sepulveda K, Lenchik L, Ivanidze J, et al. Role of imaging in the era of precision medicine. *Acad Radiol* 2017; **24**: 639–49. https://doi.org/10.1016/j.acra.2016.11.021
8. Slart RHJA, Glaudemans AWJM, Lancellotti P, Hyafil F, Blankstein R, Schwartz RG, et al. A joint procedural position statement on imaging in cardiac Sarcoidosis: from the cardiovascular and inflammation & infection committees of the European Association of nuclear medicine, the European Association of cardiovascular imaging, and the American society of nuclear cardiology. *J Nucl Cardiol* 2018; **25**: 298–319. https://doi.org/10.1007/s12350-017-1043-4
9. Slart RHJA, Glaudemans AWJM, Gheysens O, Lubberink M, Kero T, Dweck MR, et al. Procedural recommendations of cardiac PET/CT imaging: standardization in Inflammatory-, Infective-, Infiltrative-, and Innervation (4Is)-Related cardiovascular diseases: a joint collaboration of the EACVI and the EANM. *Eur J Nucl Med Mol Imaging* 2021; **48**: 1016–39. https://doi.org/10.1007/s00259-020-05066-5
10. Slart RHJA, Williams MC, Juarez-Orozco LE, Rischpler C, Dweck MR, Glaudemans AWJM, et al. Position paper of the EACVI and EANM on artificial intelligence applications in Multimodality cardiovascular imaging using SPECT/CT, PET/CT, and cardiac CT. *Eur J Nucl Med Mol Imaging* 2021; **48**: 1399–1413. https://doi.org/10.1007/s00259-021-05341-z
11. Boellaard R, Delgado-Bolton R, Oyen WJG, Giammarile F, Tatsch K, Eschner W, et al. FDG PET/CT: EANM procedure guidelines for tumour imaging: version 2.0. *Eur J Nucl Med Mol Imaging* 2015; **42**: 328–54. https://doi.org/10.1007/s00259-014-2961-x
12. Kessler L, Fragoso Costa P, Kersting D, Jentzen W, Weber M, Lüdike P, et al. Quantitative 99Mtc-DPD-SPECT/CT assessment of cardiac Amyloidosis. *J Nucl Cardiol* 2023; **30**: 101–11. https://doi.org/10.1007/s12350-022-02960-3
13. Dorbala S, Park M-A, Cuddy S, Singh V, Sullivan K, Kim S, et al. Absolute Quantitation of cardiac 99Mtc-pyrophosphate using cadmium-zinc-Telluride-based SPECT/CT . *J Nucl Med* 2021; **62**: 716–22. https://doi.org/10.2967/jnumed.120.247312
14. Hyafil F, Gimelli A, Slart RHJA, Georgoulias P, Rischpler C, Lubberink M, et al. EANM procedural guidelines for myocardial perfusion scintigraphy using cardiac-centered gamma cameras. *Eur J Hybrid Imaging* 2019; **3**(1): 11. https://doi.org/10.1186/s41824-019-0058-2
15. Karakatsanis NA, Lodge MA, Tahari AK, Zhou Y, Wahl RL, Rahmim A. Dynamic whole-body PET parametric imaging: I. concept, acquisition protocol optimization and clinical application. *Phys Med Biol* 2013; **58**: 7391–7418. https://doi.org/10.1088/0031-9155/58/20/7391
16. Hutton BF, Erlandsson K, Thielemans K. Advances in clinical molecular imaging instrumentation. *Clin Transl Imaging* 2018; **6**: 31–45. https://doi.org/10.1007/s40336-018-0264-0
17. Karakatsanis NA, Zhou Y, Lodge MA, Casey ME, Wahl RL, Zaidi H, et al. Generalized whole-body Patlak parametric imaging for enhanced Quantification in clinical PET. *Phys Med Biol* 2015; **60**: 8643–73. https://doi.org/10.1088/0031-9155/60/22/8643
18. Patlak CS, Blasberg RG. Graphical evaluation of blood-to-brain transfer constants from multiple-time uptake data. *J Cereb Blood Flow Metab* 1985; **5**: 584–90. https://doi.org/10.1038/jcbfm.1985.87
19. Dias AH, Pedersen MF, Danielsen H, Munk OL, Gormsen LC. Correction to: clinical feasibility and impact of fully automated Multiparametric PET imaging using direct Patlak reconstruction: evaluation of 103 dynamic whole-body 18F-FDG PET/CT scans. *Eur J Nucl Med Mol Imaging* 2021; **48**(3). https://doi.org/10.1007/s00259-021-05225-2
20. Hoekstra CJ, Hoekstra OS, Stroobants SG, Vansteenkiste J, Nuyts J, Smit EF, et al. Methods to monitor response to chemotherapy in non-small cell lung cancer with 18F-FDG PET. *J Nucl Med* 2002; **43**: 1304–9.
21. Slart RHJA, Tsoumpas C, Glaudemans AWJM, Noordzij W, Willemsen ATM, Borra RJH, et al. Long axial field of view PET scanners: a road map to implementation and new possibilities. *Eur J Nucl Med Mol*

Imaging 2021; **48**: 4236–45. https://doi.org/10.1007/s00259-021-05461-6
22. Vandenberghe S, Moskal P, Karp JS. State of the art in total body PET. *EJNMMI Phys* 2020; **7**(1): 35. https://doi.org/10.1186/s40658-020-00290-2
23. Spencer BA, Berg E, Schmall JP, Omidvari N, Leung EK, Abdelhafez YG, et al. Performance evaluation of the uEXPLORER total-body PET/CT scanner based on NEMA NU 2-2018 with additional tests to characterize PET scanners with a long axial field of view. *J Nucl Med* 2021; **62**: 861–70. https://doi.org/10.2967/jnumed.120.250597
24. Prenosil GA, Sari H, Fürstner M, Afshar-Oromieh A, Shi K, Rominger A, et al. Performance characteristics of the Biograph vision Quadra PET/CT system with a long axial field of view using the NEMA NU 2-2018 standard. *J Nucl Med* 2022; **63**: 476–84. https://doi.org/10.2967/jnumed.121.261972
25. Rodriguez JA, Selvaraj S, Bravo PE. Potential cardiovascular applications of total-body PET imaging. *PET Clin* 2021; **16**: 129–36. https://doi.org/10.1016/j.cpet.2020.09.004
26. Surti S, Pantel AR, Karp JS. Total body PET: Why, how, what for? *IEEE Trans Radiat Plasma Med Sci* 2020; **4**: 283–92. https://doi.org/10.1109/trpms.2020.2985403
27. Riegler G, Karanikas G, Rausch I, Hirtl A, El-Rabadi K, Marik W, et al. Influence of PET reconstruction technique and matrix size on qualitative and quantitative assessment of lung lesions on [18F]-FDG-PET: A prospective study in 37 cancer patients. *Eur J Radiol* 2017; **90**: 20–26. https://doi.org/10.1016/j.ejrad.2017.02.023
28. Jaskowiak CJ, Bianco JA, Perlman SB, Fine JP. Influence of reconstruction Iterations on 18F-FDG PET/CT standardized uptake values. *J Nucl Med* 2005; **46**: 424–28.
29. Vennart NJ, Bird N, Buscombe J, Cheow HK, Nowosinska E, Heard S. Optimization of PET/CT image quality using the GE 'sharp IR' point-spread function reconstruction algorithm. *Nucl Med Commun* 2017; **38**: 471–79. https://doi.org/10.1097/MNM.0000000000000669
30. Deidda D, Akerele MI, Aykroyd RG, Dweck MR, Ferreira K, Forsythe RO, et al. Improved identification of abdominal aortic aneurysm using the Kernelized expectation maximization algorithm. *Philos Trans A Math Phys Eng Sci* 2021; **379**(2200): 20200201. https://doi.org/10.1098/rsta.2020.0201
31. Deidda D, Karakatsanis NA, Robson PM, Tsai Y-J, Efthimiou N, Thielemans K, et al. Hybrid PET-MR list-mode Kernelized expectation maximization reconstruction. *Inverse Problems* 2019; **35**: 044001. https://doi.org/10.1088/1361-6420/ab013f
32. Nensa F, Bamberg F, Rischpler C, Menezes L, Poeppel TD, la Fougère C, et al. Hybrid cardiac imaging using PET/MRI: a joint position statement by the European society of cardiovascular Radiology (ESCR) and the European Association of nuclear medicine (EANM). *Eur Radiol* 2018; **28**: 4086–4101. https://doi.org/10.1007/s00330-017-5008-4
33. Imbert L, Poussier S, Franken PR, Songy B, Verger A, Morel O, et al. Compared performance of high-sensitivity cameras dedicated to myocardial perfusion SPECT: A comprehensive analysis of phantom and human images. *J Nucl Med* 2012; **53**: 1897–1903. https://doi.org/10.2967/jnumed.112.107417
34. Hedeer F, Akil S, Oddstig J, Hindorf C, Arheden H, Carlsson M, et al. Diagnostic accuracy for CZT gamma camera compared to conventional gamma camera technique with myocardial perfusion single-photon emission computed tomography: assessment of myocardial infarction and function. *J Nucl Cardiol* 2023. https://doi.org/10.1007/s12350-022-03185-0
35. Paravastu SS, Theng EH, Morris MA, Grayson P, Collins MT, Maass-Moreno R, et al. Artificial intelligence in vascular-PET: Translational and clinical applications. *PET Clin* 2022; **17**: 95–113. https://doi.org/10.1016/j.cpet.2021.09.003
36. Wasserthal J, Breit H-C, Meyer MT, Pradella M, Hinck D, Sauter AW, et al. Totalsegmentator: robust Segmentation of 104 anatomic structures in CT images. *Radiology: Artificial Intelligence* 2023; **5**(5). https://doi.org/10.1148/ryai.230024
37. Sundar LKS, Yu J, Muzik O, Kulterer OC, Fueger B, Kifjak D, et al. Fully automated, semantic Segmentation of whole-body 18F-FDG PET/CT images based on data-centric artificial intelligence . *J Nucl Med* 2022; **63**: 1941–48. https://doi.org/10.2967/jnumed.122.264063
38. Aerts HJWL. The potential of Radiomic-based Phenotyping in precision medicine: A review. *JAMA Oncol* 2016; **2**: 1636–42. https://doi.org/10.1001/jamaoncol.2016.2631
39. Libby P. The changing landscape of Atherosclerosis. *Nature* 2021; **592**: 524–33. https://doi.org/10.1038/s41586-021-03392-8
40. Rominger A, Saam T, Wolpers S, Cyran CC, Schmidt M, Foerster S, et al. 18F-FDG PET/CT identifies patients at risk for future vascular events in an otherwise asymptomatic cohort with neoplastic disease. *J Nucl Med* 2009; **50**: 1611–20. https://doi.org/10.2967/jnumed.109.065151
41. Reijrink M, de Boer SA, te Velde-Keyzer CA, Sluiter JKE, Pol RA, Heerspink HJL, et al. Of systemic Atherosclerosis progression: A longitudinal descriptive imaging study in patients with type 2 diabetes mellitus. *J Nucl Cardiol* 2022; **29**: 1702–9. https://doi.org/10.1007/s12350-021-02781-w
42. Dweck MR, Chow MWL, Joshi NV, Williams MC, Jones C, Fletcher AM, et al. Coronary arterial 18F-sodium fluoride uptake: A novel marker of plaque biology. *J Am Coll Cardiol* 2012; **59**: 1539–48. https://doi.org/10.1016/j.jacc.2011.12.037
43. Joshi NV, Vesey AT, Williams MC, Shah ASV, Calvert PA, Craighead FHM, et al. 18F-fluoride positron emission tomography for identification of ruptured and high-risk coronary Atherosclerotic plaques: a prospective clinical trial. *The Lancet* 2014; **383**: 705–13. https://doi.org/10.1016/S0140-6736(13)61754-7
44. McKenney-Drake ML, Moghbel MC, Paydary K, Alloosh M, Houshmand S, Moe S, et al. 18F-Naf and 18F-FDG as molecular probes in the evaluation of Atherosclerosis. *Eur J Nucl Med Mol Imaging* 2018; **45**: 2190–2200. https://doi.org/10.1007/s00259-018-4078-0
45. on behalf of the Cardiovascular Committee of the European Association of Nuclear Medicine (EANM), Bucerius J, Hyafil F, Verberne HJ, Slart RHJA, Lindner O, et al. Position paper of the cardiovascular committee of the European Association of nuclear medicine (EANM) on PET imaging of Atherosclerosis. *Eur J Nucl Med Mol Imaging* 2016; **43**: 780–92. https://doi.org/10.1007/s00259-015-3259-3
46. Saboury B, Edenbrandt L, Piri R, Gerke O, Werner T, Arbab-Zadeh A, et al. Alavi–Carlsen calcification score (ACCS): A simple measure of global cardiac Atherosclerosis burden. *Diagnostics (Basel)* 2021; **11**(8): 1421. https://doi.org/10.3390/diagnostics11081421
47. Tzolos E, Kwiecinski J, Lassen ML, Cadet S, Adamson PD, Moss AJ, et al. Observer Repeatability and Interscan reproducibility of 18F-sodium fluoride coronary Microcalcification activity. *J Nucl Cardiol* 2022; **29**: 126–35. https://doi.org/10.1007/s12350-020-02221-1
48. Kwiecinski J, Wolny R, Chwala A, Slomka P. Advances in the assessment of coronary artery disease activity with PET/CT and CTA. *Tomography* 2023; **9**: 328–41. https://doi.org/10.3390/tomography9010026
49. Mézquita AJV, Biavati F, Falk V, Alkadhi H, Hajhosseiny R, Maurovich-Horvat P, et al. Clinical quantitative coronary artery

stenosis and coronary Atherosclerosis imaging: a consensus statement from the quantitative cardiovascular imaging study group. *Nat Rev Cardiol* 2023; **20**: 696–714. https://doi.org/10.1038/s41569-023-00880-4
50. Naeger DM, Behr SC. PET/MR imaging: current and future applications for cardiovascular disease. *Magn Reson Imaging Clin N Am* 2015; **23**: 95–103. https://doi.org/10.1016/j.mric.2014.09.006
51. Banerjee S. Superficial femoral artery is not left anterior descending artery. *Circulation* 2016; **134**: 901–3. https://doi.org/10.1161/CIRCULATIONAHA.116.023690
52. Lawton JS, Tamis-Holland JE, Bangalore S, Bates ER, Beckie TM, Bischoff JM. ACC/AHA/SCAI guideline for coronary artery Revascularization: A report of the American college of cardiology/American heart Association joint committee on clinical practice guidelines. *Circulation* 2022; **145**: e18–114. https://doi.org/10.1161/CIR.0000000000001060
53. Knuuti J, Wijns W, Saraste A, Capodanno D, Barbato E, Funck-Brentano C, et al. ESC guidelines for the diagnosis and management of chronic coronary syndromes: the task force for the diagnosis and management of chronic coronary syndromes of the European society of cardiology (ESC). *Eur Heart J* 2020; **41**: 407–77.
54. Maron DJ, Hochman JS, Reynolds HR, Bangalore S, O'Brien SM, Boden WE, et al. Initial invasive or conservative strategy for stable coronary disease. *N Engl J Med* 2020; **382**: 1395–1407. https://doi.org/10.1056/NEJMoa1915922
55. Van Tosh A, Nichols KJ. SPECT measurements of myocardial blood flow and flow Reserve: from development to implementation. *J Nucl Cardiol* 2023; **30**: 1437–42. https://doi.org/10.1007/s12350-023-03273-9
56. D'Antonio A, Assante R, Zampella E, Mannarino T, Buongiorno P, Cuocolo A, et al. Myocardial blood flow evaluation with dynamic cadmium-zinc-Telluride single-photon emission computed tomography: bright and dark sides. *Diagnostic and Interventional Imaging* 2023; **104**: 323–29. https://doi.org/10.1016/j.diii.2023.02.001
57. Tang X, Dai N, Zhang B, Cai H, Huo Y, Yang M, et al. Comparison of 2d-QCA, 3d-QCA and coronary angiography derived FFR in predicting myocardial ischemia assessed by CZT-SPECT MPI. *J Nucl Cardiol* 2023. https://doi.org/10.1007/s12350-023-03240-4
58. Panjer M, Dobrolinska M, Wagenaar NRL, Slart RHJA. Diagnostic accuracy of dynamic CZT-SPECT in coronary artery disease. A systematic review and meta-analysis. *J Nucl Cardiol* 2022; **29**: 1686–97. https://doi.org/10.1007/s12350-021-02721-8
59. Cardiovascular Committee of the European Association of Nuclear Medicine (EANM), Sciagrà R, Lubberink M, Hyafil F, Saraste A, Slart RHJA, et al. EANM procedural guidelines for PET/CT quantitative myocardial perfusion imaging. *Eur J Nucl Med Mol Imaging* 2021; **48**: 1040–69. https://doi.org/10.1007/s00259-020-05046-9
60. Santarelli MF, Genovesi D, Scipioni M, Positano V, Favilli B, Giorgetti A, et al. Cardiac Amyloidosis characterization by kinetic model fitting on [18F]Florbetaben PET images. *J Nucl Cardiol* 2022; **29**: 1919–32. https://doi.org/10.1007/s12350-021-02608-8
61. Li Y, Zhang W, Wu H, Liu G. Advanced tracers in PET imaging of cardiovascular disease. *BioMed Research International* 2014; **2014**: 1–13. https://doi.org/10.1155/2014/504532
62. Maddahi J, Packard RRS. Cardiac PET perfusion tracers: Current status and future directions. *Semin Nucl Med* 2014; **44**: 333–43. https://doi.org/10.1053/j.semnuclmed.2014.06.011
63. Polycarpou I, Soultanidis G, Tsoumpas C. Synergistic motion compensation strategies for positron emission tomography when acquired simultaneously with magnetic resonance imaging. *Philos Trans A Math Phys Eng Sci* 2021; **379**(2204): 20200207. https://doi.org/10.1098/rsta.2020.0207
64. Garcia-Pavia P, Rapezzi C, Adler Y, Arad M, Basso C, Brucato A, et al. Diagnosis and treatment of cardiac Amyloidosis: a position statement of the ESC working group on myocardial and Pericardial diseases. *Eur Heart J* 2021; **42**: 1554–68. https://doi.org/10.1093/eurheartj/ehab072
65. Tsoi MR, Lin JH, Patel AR. Emerging therapies for Transthyretin Amyloidosis. *Curr Oncol Rep* 2023; **25**: 549–58. https://doi.org/10.1007/s11912-023-01397-2
66. Dorbala S, Ando Y, Bokhari S, Dispenzieri A, Falk RH, Ferrari VA, et al. ASNC/AHA/ASE/EANM/HFSA/ISA/SCMR/SNMMI expert consensus recommendations for Multimodality imaging in cardiac Amyloidosis: part 1 of 2—evidence base and standardized methods of imaging. *Circ Cardiovasc Imaging* 2021; **14**(7): e000029. https://doi.org/10.1161/HCI.0000000000000029
67. Fontana M, Martinez-Naharro A, Chacko L, Rowczenio D, Gilbertson JA, Whelan CJ, et al. Reduction in CMR derived extracellular volume with Patisiran indicates cardiac Amyloid regression. *JACC: Cardiovascular Imaging* 2021; **14**: 189–99. https://doi.org/10.1016/j.jcmg.2020.07.043
68. Rettl R, Wollenweber T, Duca F, Binder C, Cherouny B, Dachs T-M, et al. Monitoring Tafamidis treatment with quantitative SPECT/CT in Transthyretin Amyloid cardiomyopathy. *Eur Heart J Cardiovasc Imaging* 2023; **24**: 1019–30. https://doi.org/10.1093/ehjci/jead030
69. Papathanasiou M, Kessler L, Bengel FM, Jakstaite A-M, Kersting D, Varasteh Z, et al. Regression of myocardial 99Mtc-DPD uptake after Tafamidis treatment of cardiac Transthyretin Amyloidosis. *J Nucl Med* 2023; **64**: 1083–86. https://doi.org/10.2967/jnumed.122.265352
70. Castaño A, DeLuca A, Weinberg R, Pozniakoff T, Blaner WS, Pirmohamed A, et al. Serial scanning with technetium pyrophosphate (99Mtc-PYP) in advanced ATTR cardiac Amyloidosis. *J Nucl Cardiol* 2016; **23**: 1355–63. https://doi.org/10.1007/s12350-015-0261-x
71. Zhao M, Calabretta R, Yu J, Binder P, Hu S, Hacker M, et al. Nuclear molecular imaging of disease burden and response to treatment for cardiac Amyloidosis. *Biology (Basel)* 2022; **11**(10): 1395. https://doi.org/10.3390/biology11101395
72. Slart R, Glaudemans A, Hazenberg BPC, Noordzij W. Imaging cardiac Innervation in Amyloidosis. *J Nucl Cardiol* 2019; **26**: 174–87. https://doi.org/10.1007/s12350-017-1059-9
73. Ramsay SC, Cuscaden C. The current status of quantitative SPECT/CT in the assessment of Transthyretin cardiac Amyloidosis. *J Nucl Cardiol* 2020; **27**: 1464–68. https://doi.org/10.1007/s12350-019-01935-1
74. Kim SH, Kim YS, Kim S-J. Diagnostic performance of PET for detection of cardiac Amyloidosis: A systematic review and meta-analysis. *J Cardiol* 2020; **76**: 618–25. https://doi.org/10.1016/j.jjcc.2020.07.003
75. Rosengren S, Skibsted Clemmensen T, Tolbod L, Granstam S-O, Eiskjær H, Wikström G, et al. Diagnostic accuracy of [^{11}C]PIB positron emission tomography for detection of cardiac Amyloidosis. *JACC Cardiovasc Imaging* 2020; **13**: 1337–47. https://doi.org/10.1016/j.jcmg.2020.02.023
76. Antoni G, Lubberink M, Estrada S, Axelsson J, Carlson K, Lindsjö L, et al. In vivo visualization of Amyloid deposits in the heart with 11 C-PIB^{B} and PET. *J Nucl Med* 2013; **54**: 213–20. https://doi.org/10.2967/jnumed.111.102053
77. Bi X, Xu B, Liu J, Wang G, An J, Zhang X, et al. Diagnostic value of 11C-PIB PET/MR in cardiac Amyloidosis. *Front Cardiovasc*

Med 2022; **9**. https://doi.org/10.3389/fcvm.2022.830572
78. Pilebro B, Arvidsson S, Lindqvist P, Sundström T, Westermark P, Antoni G, et al. Positron emission tomography (PET) utilizing Pittsburgh compound B (PIB) for detection of Amyloid heart deposits in hereditary Transthyretin Amyloidosis (ATTR). *J Nucl Cardiol* 2018; **25**: 240–48. https://doi.org/10.1007/s12350-016-0638-5
79. Takasone K, Katoh N, Takahashi Y, Abe R, Ezawa N, Yoshinaga T, et al. Non-invasive detection and differentiation of cardiac Amyloidosis using 99m Tc-^{Pyr}Ophosphate scintigraphy and 11 C-pi^{Tt}Sburgh compound B PET imaging . *Amyloid* 2020; **27**: 266–74. https://doi.org/10.1080/13506129.2020.1798223
80. Trivieri MG, Dweck MR, Abgral R, Robson PM, Karakatsanis NA, Lala A, et al. ^{18}F-sodium fluoride PET/MR for the assessment of cardiac Amyloidosis. *J Am Coll Cardiol* 2016; **68**: 2712–14. https://doi.org/10.1016/j.jacc.2016.09.953
81. Abulizi M, Sifaoui I, Wuliya-Gariepy M, Kharoubi M, Israël J-M, Emsen B, et al. 18F-sodium fluoride PET/MRI myocardial imaging in patients with suspected cardiac Amyloidosis. *J Nucl Cardiol* 2021; **28**: 1586–95. https://doi.org/10.1007/s12350-019-01885-8
82. Martineau P, Finnerty V, Giraldeau G, Authier S, Harel F, Pelletier-Galarneau M. Examining the sensitivity of 18F-Naf PET for the imaging of cardiac Amyloidosis. *J Nucl Cardiol* 2021; **28**: 209–18. https://doi.org/10.1007/s12350-019-01675-2
83. Andrews JPM, Trivieri MG, Everett R, Spath N, MacNaught G, Moss AJ, et al. 18F-fluoride PET/MR in cardiac Amyloid: A comparison study with aortic stenosis and Age- and sex-matched controls. *J Nucl Cardiol* 2022; **29**: 741–49. https://doi.org/10.1007/s12350-020-02356-1
84. Kircher M, Ihne S, Brumberg J, Morbach C, Knop S, Kortüm KM, et al. Detection of cardiac Amyloidosis with 18F-Florbetaben-PET/CT in comparison to echocardiography, cardiac MRI and DPD-scintigraphy. *Eur J Nucl Med Mol Imaging* 2019; **46**: 1407–16. https://doi.org/10.1007/s00259-019-04290-y
85. Law WP, Wang WYS, Moore PT, Mollee PN, Ng ACT. Cardiac Amyloid imaging with 18 F-fl^{Or}Betaben PET: A pilot study. *J Nucl Med* 2016; **57**: 1733–39. https://doi.org/10.2967/jnumed.115.169870
86. Manwani R, Page J, Lane T, Burniston M, Skillen A, Lachmann HJ, et al. A pilot study demonstrating cardiac uptake with 18F-Florbetapir PET in AL Amyloidosis patients with cardiac involvement. *Amyloid* 2018; **25**: 247–52. https://doi.org/10.1080/13506129.2018.1552852
87. Iwai K, Tachibana T, Takemura T, Matsui Y, Kitalchi M, Kawabata Y. Pathological studies on Sarcoidosis autopsy. I. Epidemiological features of 320 cases in Japan. *Pathology International* 1993; **43**: 372–76. https://doi.org/10.1111/j.1440-1827.1993.tb01148.x
88. Perry A, Vuitch F. Causes of death in patients with Sarcoidosis. A morphologic study of 38 Autopsies with Clinicopathologic correlations. *Arch Pathol Lab Med* 1995; **119**: 167–72.
89. Kim JS, Judson MA, Donnino R, Gold M, Cooper LT Jr, Prystowsky EN, et al. Cardiac Sarcoidosis. *American Heart Journal* 2009; **157**: 9–21. https://doi.org/10.1016/j.ahj.2008.09.009
90. Chareonthaitawee P, Beanlands RS, Chen W, Dorbala S, Miller EJ, Murthy VL, et al. Joint SNMMI–ASNC expert consensus document on the role of 18F-FDG PET/CT in cardiac Sarcoid detection and therapy monitoring . *J Nucl Med* 2017; **58**: 1341–53. https://doi.org/10.2967/jnumed.117.196287
91. Birnie DH, Sauer WH, Bogun F, Cooper JM, Culver DA, Duvernoy CS, et al. HRS expert consensus statement on the diagnosis and management of arrhythmias associated with cardiac Sarcoidosis. *Heart Rhythm* 2014; **11**: 1304–23. https://doi.org/10.1016/j.hrthm.2014.03.043
92. Régis C, Benali K, Rouzet F. FDG PET/CT imaging of Sarcoidosis. *Semin Nucl Med* 2023; **53**: 258–72. https://doi.org/10.1053/j.semnuclmed.2022.08.004
93. Osborne MT, Hulten EA, Singh A, Waller AH, Bittencourt MS, Stewart GC, et al. Eduction in 18F-Fluorodeoxyglucose uptake on serial cardiac positron emission tomography is associated with improved left ventricular ejection fraction in patients with cardiac Sarcoidosis. *J Nucl Cardiol* 2014; **21**: 166–74. https://doi.org/10.1007/s12350-013-9828-6
94. Kersey CB, Flaherty KR, Goldenthal IL, Bokhari S, Biviano AB. The use of serial cardiac 18F-Fluorodeoxyglucose- positron emission tomography imaging to diagnose, monitor, and tailor treatment of cardiac Sarcoidosis patients with arrhythmias: a case series and review. *Eur Heart J Case Rep* 2019; **3**: 1–7. https://doi.org/10.1093/ehjcr/ytz188
95. Waller AH, Blankstein R. Quantifying myocardial inflammation using F18-Fluorodeoxyglucose positron emission tomography in cardiac Sarcoidosis. *J Nucl Cardiol* 2014; **21**: 940–43. https://doi.org/10.1007/s12350-014-9921-5
96. Divakaran S. Radionuclide assessment of Sarcoidosis. *Cardiol Clin* 2023; **41**: 207–15. https://doi.org/10.1016/j.ccl.2023.01.009
97. Cheung E, Ahmad S, Aitken M, Chan R, Iwanochko RM, Balter M, et al. Combined simultaneous FDG-PET/MRI with T1 and T2 mapping as an imaging biomarker for the diagnosis and prognosis of suspected cardiac Sarcoidosis. *Eur J Hybrid Imaging* 2021; **5**(1): 24. https://doi.org/10.1186/s41824-021-00119-w
98. Greulich S, Gatidis S, Gräni C, Blankstein R, Glatthaar A, Mezger K, et al. Hybrid cardiac magnetic resonance/Fluorodeoxyglucose positron emission tomography to differentiate active from chronic cardiac Sarcoidosis. *JACC Cardiovasc Imaging* 2022; **15**: 445–56. https://doi.org/10.1016/j.jcmg.2021.08.018
99. Olivero R, Garcia JR, Bassa P, Garcia P, Riera E, Maceira A. Early detection/diagnosis of cardiac Sarcoidosis in inflammatory stage on cardiac 18F-FDG PET/MRI. A case report. *Rev Esp Med Nucl Imagen Mol (Engl Ed)* 2021. https://doi.org/10.1016/j.remn.2021.01.001
100. Lapa C, Reiter T, Kircher M, Schirbel A, Werner RA, Pelzer T, et al. Somatostatin receptor based PET/CT in patients with the suspicion of cardiac Sarcoidosis: an initial comparison to cardiac MRI. *Oncotarget* 2016; **7**: 77807–14. https://doi.org/10.18632/oncotarget.12799
101. Mushari NA, Soultanidis G, Duff L, Trivieri MG, Fayad ZA, Robson P, et al. Exploring the utility of Radiomic feature extraction to improve the diagnostic accuracy of cardiac Sarcoidosis using FDG PET. *Front Med (Lausanne)* 2022; **9**: 840261. https://doi.org/10.3389/fmed.2022.840261
102. Mushari NA, Soultanidis G, Duff L, Trivieri MG, Fayad ZA, Robson PM, et al. n.d.).(Exploring the utility of cardiovascular magnetic resonance Radiomic feature extraction for evaluation of cardiac Sarcoidosis. *Diagnostics*; **13**: 1865. https://doi.org/10.3390/diagnostics13111865
103. Sharma A, Okada DR, Yacoub H, Chrispin J, Bokhari S. Diagnosis of cardiac Sarcoidosis: an era of paradigm shift. *Ann Nucl Med* 2020; **34**: 87–93. https://doi.org/10.1007/s12149-019-01431-z
104. Dejaco C, Ramiro S, Duftner C, Besson FL, Bley TA, Blockmans D, et al. EULAR recommendations for the use of imaging in large vessel vasculitis in clinical practice. *Ann Rheum Dis* 2018; **77**: 636–43. https://doi.org/10.1136/annrheumdis-2017-212649
105. Slart RHJA, Writing group, Reviewer group, Members of EANM Cardiovascular, Members of EANM Infection &

Inflammation, Members of Committees, SNMMI Cardiovascular, et al. FDG-PET/CT(A) imaging in large vessel vasculitis and Polymyalgia Rheumatica: joint procedural recommendation of the EANM, SNMMI, and the PET interest group (PIG), and endorsed by the ASNC. *Eur J Nucl Med Mol Imaging* 2018; **45**: 1250–69. https://doi.org/10.1007/s00259-018-3973-8

106. Gheysens O, Jamar F, Glaudemans AWJM, Yildiz H, van der Geest KSM. Semi-quantitative and quantitative [^{18}F]FDG-PET/CT indices for diagnosing large vessel vasculitis: A critical review. *Diagnostics (Basel)* 2021; **11**(12): 2355. https://doi.org/10.3390/diagnostics11122355
107. Stellingwerff MD, Brouwer E, Lensen K-JDF, Rutgers A, Arends S, van der Geest KSM, et al. Different scoring methods of FDG PET/CT in giant cell arteritis. *Medicine (Baltimore)* 2015; **94**(37): e1542. https://doi.org/10.1097/MD.0000000000001542
108. Duff LM, Scarsbrook AF, Ravikumar N, Frood R, van Praagh GD, Mackie SL, et al. An automated method for Artifical intelligence assisted diagnosis of active Aortitis using Radiomic analysis of FDG PET-CT images. *Biomolecules* 2023; **13**(2): 343. https://doi.org/10.3390/biom13020343
109. Duff L, Scarsbrook AF, Mackie SL, Frood R, Bailey M, Morgan AW, et al. A methodological framework for AI-assisted diagnosis of active Aortitis using Radiomic analysis of FDG PET-CT images: initial analysis. *J Nucl Cardiol* 2022; **29**: 3315–31. https://doi.org/10.1007/s12350-022-02927-4
110. Moreel L, Coudyzer W, Boeckxstaens L, Betrains A, Molenberghs G, Vanderschueren S, et al. Pos0217 association between vascular Fdg uptake and aortic dimensions in giant cell arteritis: A prospective study. *Ann Rheum Dis* 2023; **82**: 335.. https://doi.org/10.1136/annrheumdis-2023-eular.1559
111. de Boysson H, Liozon E, Lambert M, Parienti J-J, Artigues N, Geffray L, et al. 18F-Fluorodeoxyglucose positron emission tomography and the risk of subsequent aortic complications in giant-cell arteritis: A multicenter cohort of 130 patients. *Medicine (Baltimore)* 2016; **95**(26): e3851. https://doi.org/10.1097/MD.0000000000003851
112. de Boysson H, Aide N, Liozon E, Lambert M, Parienti J-J, Monteil J, et al. Repetitive 18F-FDG-PET/CT in patients with large-vessel giant-cell arteritis and controlled disease. *European Journal of Internal Medicine* 2017; **46**: 66–70. https://doi.org/10.1016/j.ejim.2017.08.013
113. van Praagh GD, Nienhuis PH, de Jong DM, Reijrink M, van der Geest KSM, Brouwer E, et al. Toward reliable uptake Metrics in large vessel vasculitis studies. *Diagnostics* 2021; **11**: 1986. https://doi.org/10.3390/diagnostics11111986
114. Nienhuis PH, van Praagh GD, Glaudemans AWJM, Brouwer E, Slart RHJA. A review on the value of imaging in differentiating between large vessel vasculitis and Atherosclerosis. *J Pers Med* 2021; **11**(3): 236. https://doi.org/10.3390/jpm11030236
115. van der Geest KSM, Treglia G, Glaudemans AWJM, Brouwer E, Sandovici M, Jamar F, et al. Diagnostic value of [18F]FDG-PET/CT for treatment monitoring in large vessel vasculitis: a systematic review and meta-analysis. *Eur J Nucl Med Mol Imaging* 2021; **48**: 3886–3902. https://doi.org/10.1007/s00259-021-05362-8
116. Murillo H, Restrepo CS, Marmol-Velez JA, Vargas D, Ocazionez D, Martinez-Jimenez S, et al. Infectious diseases of the heart: pathophysiology. *Clinical and Imaging Overview RadioGraphics* 2016; **36**: 963–83. https://doi.org/10.1148/rg.2016150225
117. Arnon-Sheleg E, Keidar Z. Vascular graft infection imaging. *Semin Nucl Med* 2023; **53**: 70–77. https://doi.org/10.1053/j.semnuclmed.2022.08.006
118. Ferro P, Boni R, Slart RH, Erba PA. Imaging of Endocarditis and cardiac device-related infections: an update. *Semin Nucl Med* 2023; **53**: 184–98. https://doi.org/10.1053/j.semnuclmed.2023.01.001
119. Lauri C, Iezzi R, Rossi M, Tinelli G, Sica S, Signore A, et al. Imaging modalities for the diagnosis of vascular graft infections: A consensus paper amongst different specialists. *JCM* 2020; **9**: 1510. https://doi.org/10.3390/jcm9051510
120. Kirkbride RR, Rawal B, Mirsadraee S, Galperin-Aizenberg M, Wechalekar K, Ridge CA, et al. Imaging of cardiac infections: A comprehensive review and investigation Flowchart for diagnostic Workup. *J Thorac Imaging* 2021; **36**: W70–88. https://doi.org/10.1097/RTI.0000000000000552
121. Rojoa D, Kontopodis N, Antoniou SA, Ioannou CV, Antoniou GA. 18F-FDG PET in the diagnosis of vascular prosthetic graft infection: A diagnostic test accuracy meta-analysis. *European Journal of Vascular and Endovascular Surgery* 2019; **57**: 292–301. https://doi.org/10.1016/j.ejvs.2018.08.040
122. Jiménez-Ballvé A, Pérez-Castejón MJ, Delgado-Bolton RC, Sánchez-Enrique C, Vilacosta I, Vivas D, et al. Assessment of the diagnostic accuracy of 18F-FDG PET/CT in prosthetic infective Endocarditis and cardiac Implantable electronic device infection: comparison of different interpretation criteria. *Eur J Nucl Med Mol Imaging* 2016; **43**: 2401–12. https://doi.org/10.1007/s00259-016-3463-9
123. Swart LE, Gomes A, Scholtens AM, Sinha B, Tanis W, Lam MGEH, et al. Improving the diagnostic performance of 18F-Fluorodeoxyglucose positron-emission tomography/computed tomography in prosthetic heart valve Endocarditis. *Circulation* 2018; **138**: 1412–27. https://doi.org/10.1161/CIRCULATIONAHA.118.035032
124. Hove D ten, Wahadat AR, Slart RHJA, Wouthuyzen-Bakker M, Mecozzi G, Damman K, et al. The Additive Value of Semi-Quantitative Analysis of 18F-FDG PET/CT For The Diagnosis of Device Related Infections In Patients With A Left Ventricular Assist Device. *Eur Heart J Cardiovasc Imaging* 2022: jeac260. https://doi.org/10.21203/rs.3.rs-990449/v1
125. Chang C-Y, Chang C-P, Shih C-C, Yang B-H, Cheng C-Y, Chang C-W, et al. Added value of dual-time-point 18F-FDG PET/CT with delayed imaging for detecting aortic graft infection: an observational study. *Medicine (Baltimore)* 2015; **94**(27): e1124. https://doi.org/10.1097/MD.0000000000001124
126. Signore A, Jamar F, Israel O, Buscombe J, Martin-Comin J, Lazzeri E. Clinical indications, image acquisition and data interpretation for white blood cells and anti-granulocyte Monoclonal antibody scintigraphy: an EANM procedural guideline. *Eur J Nucl Med Mol Imaging* 2018; **45**: 1816–31. https://doi.org/10.1007/s00259-018-4052-x
127. Sheikh A. Evolution of Quantification in clinical nuclear medicine: A brief overview of salient uses and upcoming trends. *J Nucl Med Radiat Ther* 2018; **09**: 05. https://doi.org/10.4172/2155-9619.1000375
128. Hatt M, Krizsan AK, Rahmim A, Bradshaw TJ, Costa PF, Forgacs A, et al. Joint EANM/SNMMI guideline on Radiomics in nuclear medicine: jointly supported by the EANM physics committee and the SNMMI physics. *Eur J Nucl Med Mol Imaging* 2023; **50**: 352–75. https://doi.org/10.1007/s00259-022-06001-6